1-s2.0-S2352938520300690-main_1.pdf

by

Submission date: 03-Feb-2022 11:48AM (UTC+0700)
Submission ID: 1753943193
File name: 1-s2.0-S2352938520300690-main_1.pdf (2.45M)
Word count: 8974
Character count: 46064

Remote Sensing Applications: Society and Environment 19 (2020) 100335

Contents lists available at ScienceDirect

Remote Sensing Applications: Society and Environment

journal homepage: http://www.elsevier.com/locate/rsase

Analyses of inter-class spectral separability and classification accuracy of benthic habitat mapping using multispectral image

Pramaditya Wicaksono [a, *], Prama Ardha Aryaguna [b]

[a] Department of Geographic Information Science, Faculty of Geography, Universitas Gadjah Mada, Yogyakarta, 55281, Indonesia
[b] Faculty of Engineering, Universitas Esa Unggul, Jakarta, 11510, Indonesia

ARTICLE INFO

Keywords:
Separability
WorldView-2
Benthic
Classification accuracy

ABSTRACT

Theoretically, spectral separability will greatly affect the accuracy of multispectral classification. This study aims to understand the relationship between the inter-class spectral separability and the accuracy of benthic habitat classification using a WorldView-2 multispectral image. The study area for this research is Kemujan Island, Jepara Regency, Central Java Province, Indonesia. The datasets used are sunglint-corrected bands, Principle Component Analysis (PCA)-derived bands, vegetation indices, and filter occurrence bands. Benthic habitat field data were obtained through a photo-transect survey technique and were used to construct nine levels of benthic habitat hierarchical classification schemes. We used maximum likelihood (ML) and random forest (RF) as the classification algorithms. Spectral separability was calculated using the Jeffries-Matusita separability analysis algorithm. The results from both RF and ML showed that the increased number of class pairs with spectral separability less than 1.0 ($S_{<1.0}$) decreased the OA and an increased number of class pairs with $S_{>1.0\text{-}1.9}$ increased the OA. Especially for scheme Level 1 with the greatest number of classes, an increased number of class pairs with $S_{>1.9}$ to is required to improve the OA. This has proven that the spectral separability between classes does affect the accuracy of benthic habitat classification and there is a significant relationship between spectral separability and the accuracy of benthic habitat classification.

1. Introduction

Benthic habitat mapping is generally done through the integration of remote sensing and field data (Kutser et al., 2020). The integration process can be done through, among other methods, pixel-based digital classification (Oppelt et al., 2012) (Wicaksono et al., 2019), Object-based Image Analysis (OBIA) (Phinn et al., 2012) (Roelfsema et al., 2013), derivative analysis (Kutser et al., 2006) (Oppelt et al., 2012) and empirical modeling (Yang et al., 2011) (Joyce et al., 2013) (Wicaksono and Hafizt, 2013). The per-pixel classification and OBIA are applied to map information at the categorical data level (nominal and ordinal data), whereas empirical modeling and derivative analysis are used for the mapping of benthic habitat information at the continuous data level (e.g. intervals and ratios).

In the process of digital classification of benthic habitats, training areas are generally obtained through field survey (Green et al., 2000) (Goodman et al., 2013) (Kutser et al., 2020). Visual interpretation on high spatial resolution images can be used to select the training area if done by an expert or people with high local knowledge. The spectral library can also be used to obtain pure endmember for Linear Spectral Unmixing (LSU) and Spectral Angle Mapper (SAM) (Wicaksono et al., 2019). In integrating field survey data, there is sometimes a gap between the information obtained in the field and the information recorded on the image (Hedley et al., 2012). Not all field information can be well-recognized by the sensor, especially by sensors with low spatial, spectral, and radiometric resolution. This gap is one of the factors that affect the classification accuracy of remote sensing data.

Benthic habitat is one of the objects on the earth surface that is quite difficult to identify through satellite images, due to the fact that: (1) they are located underwater, hence the influence of sunglint (Kay et al., 2009) and energy attenuation by the water column (Hedley et al., 2012) (Zoffoli et al., 2014) contributes to the overall spectral response of benthic habitat recorded by the sensor, (2) there is a wide variety of biota with very high or similar spectral response variations, which is due to the almost identical pigment composition and concentration contained by the biota (Penuelas et al., 1993) (Hochberg and Atkinson, 2000) (Oppelt et al., 2012) (Wicaksono et al., 2019). This condition results in the identification of benthic habitat variations in multispectral

* Corresponding author.
E-mail addresses: prama.wicaksono@ugm.ac.id (P. Wicaksono), prama.ardha@esaunggul.ac.id (P.A. Aryaguna).

https://doi.org/10.1016/j.rsase.2020.100335
Received 28 February 2020; Received in revised form 22 May 2020; Accepted 25 May 2020
Available online 30 May 2020

images and medium-to-low spatial resolution images being difficult, and (3) benthic habitat classification schemes used to label each field sample do not necessarily reflect or build on the maximum descriptive resolution of the remote sensing data used (Wicaksono et al., 2013). As a result, the accuracy of benthic habitat mapping is often inconsistent and very difficult to compare with one another.

Therefore, after the labeling of field samples, it is necessary to test whether the classes in the classification scheme are truly distinguishable by the spectral bands used in the classification process. One approach that can be used to test the spectral-separability between classes is by using the Jeffries-Matusita (J-M) distance method (Richards, 2013) (Eugenio et al., 2015). This method calculates the inter-class spectral separability in the classification scheme. The closer the distance or separation between classes, the more the two classes are vulnerable to being misclassified and vice versa.

The purpose of this study is to assess the relationship between the spectral separability between benthic habitat classes in different classification schemes and the resulting classification accuracy. The remote sensing image used is WorldView-2, the spectral separability was calculated using the J-M distance method, the benthic habitat classification scheme refers to the composition of the benthic habitat *in situ* constructed based on field survey, the digital classification was performed by per-pixel classification algorithms, and the relationship between inter-class spectral separability and classification accuracy was analyzed using correlation and regression analysis. OBIA was not applied in this research because the implementation of OBIA will complicate the process of quantifying the relationship between classification accuracy and inter-class spectral separability, since the accuracy from an OBIA classification result does not only rely on the spectral response difference between benthic habitats alone, but also takes into consideration their spatial aspects, e.g., texture, shape, size.

2. Study area

This research was conducted in Kemujan Island, Karimunjawa Islands, Central Java Province, Indonesia (Fig. 1). Kemujan Island was chosen as the study area because it has a complete morphological and ecological variation of benthic habitat. Kemujan is the only island in the

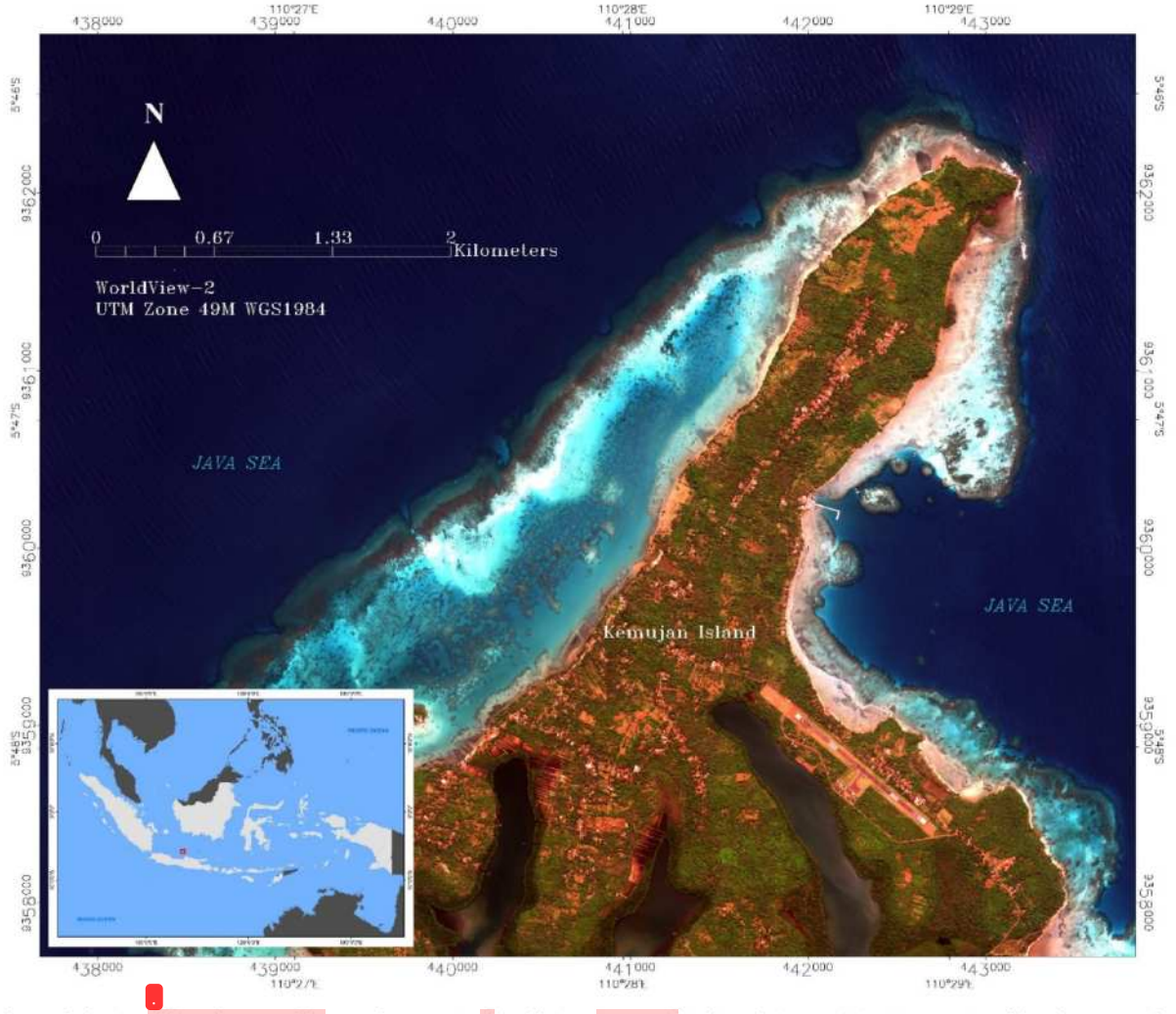

Fig. 1. The location of the study area and the true color composite of WorldView-2 image used in this study (RGB 532). (For interpretation of the references to color in this figure legend, the reader is referred to the Web version of this article.)

Karimunjawa Islands, among a few of the small islands of Indonesia, to have a complete coral reef morphology configuration of, e.g. Reef flat, back reef, lagoon, reef crest, fore reef, reef cut, spur and groove, shelf, and escarpment. In addition to having a high variety of coral reef life-forms, Kemujan Island is home to several seagrass species, e.g., *Enhalus acoroides, Thalassia hemprichii, Cymodocea rotundata*, and macroalgae, e.g., *Padina Sp., Caulerpa Sp., Sargassum Sp., Dictyota Sp., Eucheuma Sp.* Furthermore, each benthic habitat is not always found in a single homogenous cluster, instead, they are also commonly found overlapping and interleaving each other, e.g., seagrass with macroalgae and rubble, coral reefs and macroalgae, and dead coral with macroalgae, especially in the lagoon, back reef, and reef flat area, which make it challenging to map using remote sensing. Thus, Kemujan Island is well suited to test the spectral separability of benthic habitat classes. The mapping depth-limit of our study area is 17.6 m. This is based on the maximum depth of penetration of Quickbird's blue band in Karimunjawa Islands (Wicaksono and Hafizt, 2013). Quickbird blue band's (447–512 nm) has almost similar range with WV2's blue band (450–510 nm), hence their maximum DOP will be relatively similar. Although variations in water quality, sun angle, and sea conditions can cause variations in maximum depth of penetration between Quickbird's and WorldView-2 recording dates, the difference will not be significant.

3. Image data

This study used a WorldView-2 (WV2) image recorded on May 24, 2012. The WV2 image was selected to represent the state-of-the-art development of a multispectral satellite system, primarily because of the number of spectral bands capable of penetrating a body of water (Table 1). WorldView-3 (WV3) is newer, but the number of visible bands is similar to WorldView-2 and there is no available archive of WV3 images for our study area. This image has a spatial resolution of 2 m (not 1.84 m due to the off-nadir viewing angle of 14.5°), an 11-bit radiometric resolution, and has a new cyan, yellow, and red-edge band lacking in other high spatial resolution multispectral images such as Quickbird, IKONOS, PlanetScope, SkySat, and Geoeye-1. The WV2 image was acquired on LV3X and has been ortho-rectified. Fig. 1 shows the WV2 image used in this study. The overall quality of the WV2 is very good with no cloud cover and haze over optically shallow water pixels. However, sunglint is visible, especially in the reef crest, the seaward margin of the fore reef, and the optically deep water. Based on this, in addition to performing atmospheric correction, we also applied sunglint correction.

4. Methods

4.1. Field survey

A benthic habitat field survey was conducted using photo-transect techniques (Roelfsema and Phinn, 2009). The location of the transect was chosen by considering the variation of benthic habitat in the study area as observed from visual analysis of the true color composite of the WV2 image. In total, 1614 benthic photos were obtained and used as samples; 1086 and 528 samples were used as a training area for classification and accuracy assessment, respectively. Each field sample was labeled based on the composition of its benthic habitat. Benthic classes considered in this study are Coral reefs, Dead coral, Seagrass, Macroalgae, Sand, and Rubble. Each sample has nine labels of benthic habitat composition, representing different levels of information precision (Table 3).

4.2. Image corrections

Image corrections include sensor calibration, atmospheric correction, and sunglint correction. The sensor calibration was performed using the formula provided by (Updike and Comp, 2010) using absolute calibration coefficients provided in the image header to convert Digital Number (DN) to at-sensor Radiance. The atmospheric correction was done using the Dark-Object Subtraction (DOS) technique (Lantzanakis et al., 2016). The dark target to model the atmospheric offset was estimated from the optically deep-water pixel values. Sunglint correction was performed using the method developed by (Hedley et al., 2005), using an empirical model of sunglint intensity variation relationship between visible bands and near-infrared (NIR) bands. Since the WV2 image has two NIR bands, empirical modeling was run twice for each NIR band to find the best NIR band for correcting the sunglint on each visible band. The NIR band 1 was used to correct sunglint in cyan, blue, green, and red band while NIR band 2 was used to correct sunglint in the yellow and red-edge band. Afterwards, we applied water column correction to normalize the effect of water column energy attenuation in the benthic habitat reflectance. The water-depth invariant bottom index (DII) method developed by (Lyzenga, 1978) was used to perform water column correction on six sunglint-corrected bands.

4.3. Image transformations

Image transformations applied to the atmospherically corrected WV2 image are Principle Component Analysis (PCA) and vegetation index. PCA has been widely applied to remote sensing images for mapping and biophysical modeling, both terrestrial (Kattenborn et al., 2015) and underwater (Wicaksono, 2016) (Manuputty et al., 2017). PCA can improve the accuracy of classification and biophysical modeling when compared to reflectance bands, e.g. blue, green, red (Kattenborn et al., 2015)(Wicaksono, 2016) (Manuputty et al., 2017). Some of the advantages of implementing PCA include: 1) capable of producing components (PC bands), where each contains information aggregation from the input bands, so that information in each PC band is far more effective and comprehensive than a single reflectance band, 2) capable of separating information from noise, 3) more effective information on a reduced number of bands, so the resources needed for data processing and training area requirement are much lighter, and 4) minimize data redundancy commonly encountered in multispectral and hyperspectral data (Kattenborn et al., 2015)(Wicaksono, 2016).

PCA was applied to the six de-glinted reflectance bands whose land and optically-deep water pixels were masked. The masking process in PCA can improve the quality of PC bands, as it maximizes the variation of information on specific objects. PCA was also applied to the stack of vegetation indices listed in Table 2. We decided to use all PC bands in the classification processes because our experiment on only using PC bands with high eigenvalues yielded lower accuracy compared to when all PC bands were used.

The use of vegetation index in this study is interesting because vegetation index is practically effective for a land-based image processing routine since the NIR band does not penetrate water body.

Table 1
WorldView-2 image specification used in this study.

Name	WorldView-2		
Correction Level	LV3X		
Date of Acquisition	24 May 2012		
Solar Zenith	32.6°		
Off-Nadir viewing	14.5°		
Multispectral Bands	Bands	Wavelength	Coefficient of Calibration
	Cyan	400–450 nm	0.009295654
	Blue	450–510 nm	0.01783568
	Green	510–580 nm	0.01364197
	Yellow	585–625 nm	0.005829815
	Red	630–690 nm	0.01103623
	Red-edge	705–745 nm	0.005188136
	Near-IR 1	770–895 nm	0.01224380
	Near-IR 2	860–1040 nm	0.009042234
Radiometric Resolution	11 bit		

Table 2
Formula of the vegetation index used in this study. R_B = blue band, R_G = green band, R_R = red band, R_{NIR} = near-infrared band. For EVI, the value of $C1 = 6$, $C2 = 7.5$, $L = 1$, and $G = 2.5$.

No.	Vegetation index	Formula
1	SR	R_{NIR}/R_R
2	NDVI	$(R_{NIR} - R_R)/(R_{NIR} + R_R)$
3	VARI	$(R_G - R_R)/(R_G + R_R - R_B)$
4	EVI	$G\,(((R_{NIR} - R_R)/(R_{NIR} + (C1 \times R_R) - (C2 \times R_B) + L))\,(1 + L))$

However, most vegetation index also involved red band, and some even involved blue and green bands; these bands can penetrate water. Therefore, we are aware that vegetation index still provides some usable and useful information about the benthic habitat in the optically shallow water (Fig. 2). The selected vegetation indices are the Simple Ratio (SR), Normalized-Difference Vegetation Index (NDVI), Visible Atmospherically Resistant Index (VARI), and Enhanced Vegetation Index (EVI) (Table 2). SR (Birth and McVey, 1968) was chosen because it is the simplest vegetation index and its use is very easy and extensive. NDVI (Rouse et al., 1973) used in previous studies were able to improve the accuracy of benthic habitat mapping (Wicaksono, 2010). VARI (Gitelson et al., 2002) was selected because all the inputs are visible bands, so it can detect underwater object variations. EVI (Huete et al., 2002) is one of the best vegetation indices with the ability to model vegetation with high biomass. The use of blue band in EVI is expected to provide variation of benthic habitat information in the presence of strong absorption by water column and pigment contained in coral reefs, seagrass, and macroalgae.

$$B = 1/8\,((x-y)^t\,((\Sigma_x+\Sigma_y)/2)^{-1}\,(x-y)) + (1/2\ln((|(\Sigma_x+\Sigma_y)/2)|)\,/\,(|\Sigma_x|^{1/2}|\Sigma_y|^{1/2})) \quad (2)$$

4.4. Filter occurrence

Previous research has shown that texture analysis can improve the accuracy of seagrass mapping and benthic habitats (Massot-Campos et al., 2013) (Kakuta et al., 2016), which may be due to texture analysis capable of representing more complex variations of information than the spectral reflection of objects (Mumby and Edwards, 2002). In this research, texture analysis was conducted using a filter based on the first-order occurrence measure. This filter was applied on all six PC bands and resulted in filtered PC bands with the following algorithms, namely Mean (PCA-Mean), Variance (PCA-Variance), Data Range (PCA-Data range), and Skewness (PCA-Skewness) (Anys et al., 1994).

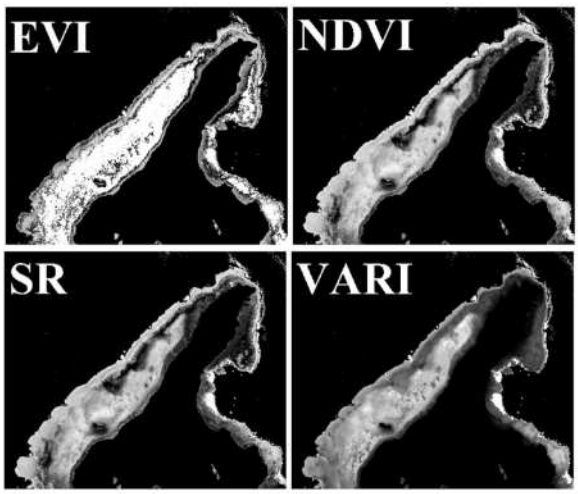

Fig. 2. Vegetation indices used in this research. These indices are still able to provide information on benthic habitat variations. Darker pixels indicate shallower waters.

4.5. J-M distance analysis

Several benthic habitat mapping works explicitly reported the use of J-M distance analysis prior to the classification process to measure the spectral separability between classes (Eugenio et al., 2015) (Eugenio et al., 2017). This analysis was used to calculate the spectral separability between classes at each benthic habitat classification scheme, using training area statistics of each class based on probability distributions. The spectral separability analysis was performed for all classification inputs listed in Table 3. The range of values generated by this method is 0.0–2.0, where a value of 0.0 means that the pair of classes have a perfect resemblance and the value of 2.0 indicates that the class pairs are completely different. Ideally, the inter-class separability value in the classification scheme used is more than 1.9. It is calculated using the followings formulas (Richards, 2013).

$$J_{xy} = 2(1-e^{-B}) \quad (1)$$

Where, x = vector of first object spectral response; y = vector of second object spectral response; Σ_x = covariance matrix of sample x; Σ_y = covariance matrix of sample y.

4.6. Image classifications

Digital classification algorithms used in this research are parametric classification maximum likelihood (ML) (Mather and Koch, 2011) and non-parametric random forest (RF) machine learning algorithm

Table 3
Input bands for ML and RF classification algorithm.

Input types	Description
Deglint[1]	6 sunglint-corrected WorldView-2 bands (cyan to red-edge)
PCA[2]	6 PC bands from the application of PCA to 6 Deglint bands[1]
DII	15 Depth-invariant bottom indices from 6 sunglint-corrected WorldView-2 bands[1]
VI[3]	Stack of 4 vegetation indices: SR, NDVI, EVI and VARI
VI-PCA	6 PC bands from the application of PCA to VI[3]
Deglint-SR	6 Deglint bands[1] and SR
Deglint-NDVI	6 Deglint bands[1] and NDVI
Deglint-EVI	6 Deglint bands[1] and EVI
Deglint-VARI	6 Deglint bands[1] and VARI
PCA-SR	6 PC bands[2] and SR
PCA-NDVI	6 PC bands[2] and NDVI
PCA-EVI	6 PC bands[2] and EVI
PCA-VARI	6 PC bands[2] and VARI
PCA-Data range	Result of filtering with Data range algorithm on 6 PC bands[2]
PCA-Mean	Result of filtering with Mean algorithm on 6 PC bands[2]
PCA-Variance	Result of filtering with Variance algorithm on 6 PC bands[2]
PCA-Skewness	Result of filtering with Skewness algorithm on 6 PC bands[2]

(Breiman and Cutler, 2011). The ML is commonly used in the classification of underwater objects (Andréfouët et al., 2003) (Pu et al., 2012) (Zapata-Ramirez et al., 2013), and RF algorithm is being used more frequently in benthic habitat mapping as well (Zhang et al., 2013) (Zhang, 2015) (Wicaksono et al., 2019). For the RF parameters, the number of trees is 100, the function to determine the number of randomly selected is square root of all features, and the function to determine the impurity in a node is Gini coefficient. The results of this study may provide a better understanding and broadly relevant information on the relationship of the accuracy of commonly and emergingly used classification algorithms with the spectral separability between benthic habitat classes in the classification scheme. The list of input bands used for image classification can be seen in Table 3.

4.7. Accuracy assessment and correlation analysis

The classification accuracy assessment was done by confusion matrix (Congalton and Green, 2008). This method produces the value of overall accuracy (OA), user's accuracy (UA) and producer's accuracy (PA). The evaluation of the classification accuracy did not only take the OA into account, but also the consistency of the UA and PA of the benthic habitat classes in the classification scheme. Pearson Product Moment correlation analysis and simple linear regression analysis were used to assess and quantify the relationship between classification OA and spectral separability between benthic habitat classes. Relationships are considered significant if it is able to surpass the threshold value of r (correlation coefficient) at 95% confidence level at a specific number of samples n. During the correlation and regression analysis, the spectral separability values are categorized into three categories: (1) less than 1 ($S_{<1.0}$), (2) between 1.0-1.9 ($S_{1.0\text{-}1.9}$), and (3) more than 1.9 ($S_{>1.9}$). Then, for each classification scheme, the number of class pairs in each category of separability were correlated to its classification OA.

5. Results

5.1. Accuracy assessment between classification schemes

Table 4 shows the hierarchical benthic habitat classification schemes constructed based on the field benthic photos collected in the field using photo-transect survey. The inter-class separability was calculated for all benthic habitat class pairs in each of these classification schemes. It is also clear that the number of training areas per class are not evenly distributed, especially at higher complexity classification schemes. This uneven training area distribution will also contribute to the classification algorithm's performance in classifying benthic habitat. The process of combining benthic habitat classes was done from an ecological point of view. The benthic habitat class mentioned first is the dominant class (>70%). The second benthic class is the less dominant (<30%). If there is a third class, the proportion with the second class is relatively similar. The final scenario of this study was to try to run the classification process using a modified classification scheme using only the constructed and non-constructed class (Level 9). The constructed class consists of benthic habitats that have pigment content (coral reef, macroalgae, seagrass), so its spectral response is primarily influenced by the variation of pigment composition and concentration (Hochberg and Atkinson, 2000). Non-constructed class consists of substrates such as sand and rubble. This class is dominated by the spectral response of calcium carbonate. Hence, the spectral response of the two classes is quite contrasting.

Fig. 3a shows the average and maximum OA of RF and ML in various benthic habitat classification schemes. RF produced higher OA than ML for each classification scheme and the difference in OA between RF and ML widens with the increasing number of classes in the classification scheme. Furthermore, there is a significant correlation between the number of classes in the classification scheme and the OA from RF and ML classification results (RF max OA, r = -0.83; RF mean OA, r = -0.77; ML max OA, r = -0.82; ML mean OA, r = -0.82). The resulting correlation is negative, which means that the more complex and the greater the number of benthic habitat classes in a classification scheme, the lower the OA produced (Fig. 3b). However, the decrease in OA in RF is not as big as ML and shows that in the use of the same remote sensing image and training area composition, RF is able to handle the classification process with various classification schemes much better than ML. This can also be used as an indicator that the machine-learning algorithm is able to handle complex classification better than parametric classification, especially in classification schemes with a large number of classes, where the composition of training areas between benthic habitat classes

Table 4
Hierarchical benthic habitat classification schemes created based on the field benthic photos collected in the field and the number of training areas for each benthic habitat class. C – coral reef, Sg – seagrass, M – macroalgae, Sd – sand, D – dead coral, R – rubble.

No	Level 1	Level 2	Level 3	Level 4	Level 5	Level 6	Level 7	Level 8	Level 9
1	M/261	M/261	M/261	M/261	M/332	M/332	M/332	Sg M/561	Constructed/958
2	M C/25	M C/25	M C/109						
3	M C D/77	M C D/84							
4	M C Sd/7								
5	M Sg/7	M Sg/16	M Sg/16						
6	M Sg Sd/9								
7	M Sd/21	M Sd/21	M Sd R/35	M Sd/71					
8	M R D/7	M R/14							
9	M R/7								
10	Sg Sd/91	Sg Sd/91	Sg Sd/91	Sg Sd/110	Sg/199	Sg/199	Sg/229		
11	Sg/89	Sg/89	Sg/89	Sg/89					
12	Sg M Sd/7	Sg M/14	Sg M/14	Sg M/30	Sg M/30	Sg M/30			
13	Sg M/7								
14	C Sd/21	C Sd R/31	C Sd R/31	C Sd R/77	C Sd R/77	C/397	C/397	C/397	
15	C R/10								
16	C/142	C/142	C/142	C/142	C/320				
17	C M/46	C M/46	C M/69	C M/178					
18	C M D/16	C M D/23							
19	C M Sd/7								
20	Sd/128	Sd/128	Sd/128	Sd/128	Sd/128	Sd/128	Sd/128	Sd/128	Non-Constructed/128
21	Sd M/36	Sd M/36	Sd M/36						
22	Sd R/16	Sd R/23	Sd C R/46						
23	Sd C R/16	Sd C R/23							
24	R C M/7								
25	R/7								
26	Sd Sg/19	Sd Sg/19	Sd Sg/19						

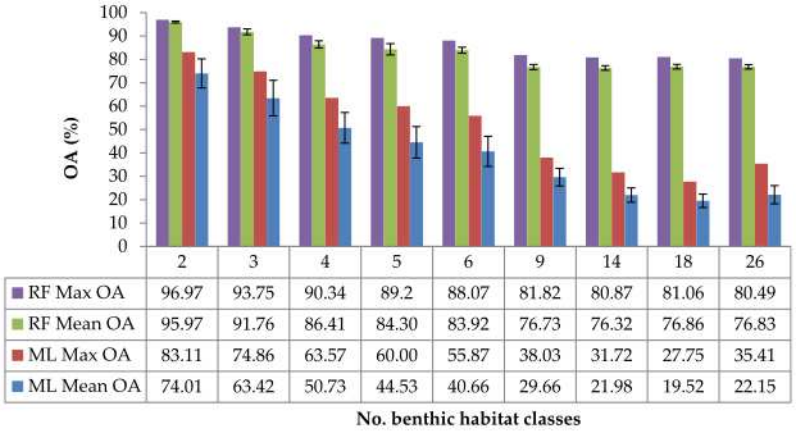

	2	3	4	5	6	9	14	18	26
RF Max OA	96.97	93.75	90.34	89.2	88.07	81.82	80.87	81.06	80.49
RF Mean OA	95.97	91.76	86.41	84.30	83.92	76.73	76.32	76.86	76.83
ML Max OA	83.11	74.86	63.57	60.00	55.87	38.03	31.72	27.75	35.41
ML Mean OA	74.01	63.42	50.73	44.53	40.66	29.66	21.98	19.52	22.15

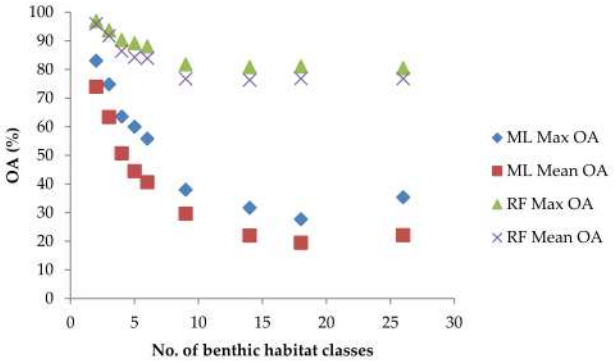

Fig. 3. (*a*) The average OA (with standard deviation) and the maximum OA of RF and ML for each classification scheme, and (*b*) The scatter plot between OA and the number of classes. There is a clear difference in the OA decrease gradient between RF and ML as the number of classes increase.

is not balanced. Several works also documented the limitation of ML in the use of non-normally distributed training samples (Su and Huang, 2009) and the superiority of machine learning compared to the parametric classification algorithm in handling complex classification issues (Zhang et al., 2013) (Wicaksono et al., 2019).

PCA-Mean produced the highest OA from Level 1 to Level 8 for ML and from Level 1 to Level 7 for RF. For ML, at Level 9, the accuracy of PCA-Mean is slightly lower than other inputs but still among the best performers. In our case, this may indicate that the combination of PCA and Mean texture analysis is effective for mapping benthic habitat at higher complexities. For RF, the highest OA of Level 8 and Level 9 scheme was obtained from PCA-SR and VI, respectively, but similarly, PCA-Mean produced among the highest OA with OA 0.6% lower than the highest OA. Nevertheless, at Level 8 and 9, all input types produced similarly high OA due to the very simple classification scheme. Also, in this research, the application of water column correction did not improve the OA of benthic habitat mapping; the resulting OA from DII in all classification schemes are comparable and relatively similar to the OA of de-glinted reflectance-based input types.

RF also produced more consistent OA for various image inputs compared to ML. The various types of inputs used do not have much impact on the OA of RF classification results, which is indicated by the low standard deviation of the average OA produced by all inputs. The range of standard deviation values for the average OA of RF is 0.90% from the Level 9 scheme to 4.91% from the Level 6 scheme. When compared to ML, different inputs produced relatively different OA,

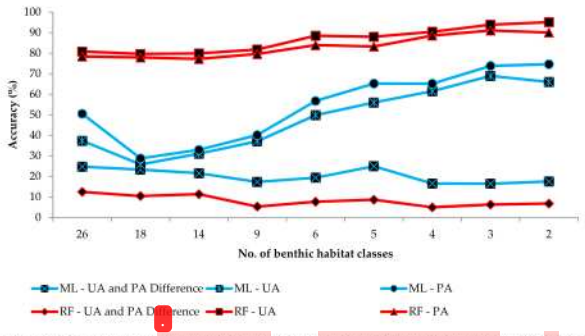

Fig. 4. The average user's accuracy (UA) and producer's accuracy (PA) of all benthic habitat classes and difference between mean UA and PA of all benthic classes per classification scheme. These values were taken from ML and RF classification results with the highest OA per classification scheme.

indicated by a wider standard deviation range between 5.82% (Level 2) and 15.52% (Level 8). This also indicates that ML is more sensitive to the selection of input bands for classification.

Fig. 4 illustrates the superiority of RF over ML based on the mean UA and PA of the classification results with the highest OA per scheme. The gap in the UA and PA of RF and ML in complex classification schemes is much greater than in simpler classification schemes. Moreover, the UA

Table 5
Correlation analysis between inter-class spectral separability and classification OA. The values of r and R^2 between the number of inter-class spectral separability per each category and OA is significant at CL 95%. NS - not significant, n - average number of class pairs belong to the category.

Maximum Likelihood											
Classification scheme		Spectral separability (mean, rounded to the nearest integer)									OA (%)	
Level	No. of class	$S_{<1.0}$			$S_{1.0-1.9}$			$S_{>1.90}$			Maximum	Mean
		n	r	R^2	n	r	R^2	n	r	R^2		
1	26	26	NS	NS	166	-0.48	0.23	133	NS	NS	35.41	22.15
2	18	32	NS	NS	118	NS	NS	3	NS	NS	27.75	19.52
3	14	22	NS	NS	66	NS	NS	3	NS	NS	31.72	21.98
4	9	13	NS	NS	23	NS	NS	1	NS	NS	38.03	29.66
5	6	5	NS	NS	10	NS	NS	0	NS	NS	55.87	40.66
6	5	2	-0.53	0.28	8	0.58	0.34	0	NS	NS	60.00	44.53
7	4	2	-0.58	0.33	4	0.58	0.33	0	NS	NS	63.57	50.73
8	3	1	-0.62	0.39	2	0.62	0.39	0	NS	NS	74.86	63.42
9	2	1	-0.49	0.24	1	0.49	0.24	0	NS	NS	83.11	74.01
Random Forest												
Classification scheme		Spectral separability (mean, rounded to the nearest integer)									OA (%)	
Level	No. of class	$S_{<1.0}$			$S_{1.0-1.9}$			$S_{>1.90}$			Maximum	Mean
		n	r	R^2	n	r	R^2	n	r	R^2		
1	26	26	NS	NS	166	-0.58	0.33	133	0.52	0.27	80.49	76.83
2	18	32	NS	NS	118	NS	NS	3	NS	NS	81.06	76.86
3	14	22	NS	NS	66	NS	NS	3	NS	NS	80.87	76.32
4	9	13	NS	NS	23	0.49	0.24	1	NS	NS	81.82	76.73
5	6	5	-0.65	0.43	10	0.68	0.47	0	NS	NS	88.07	83.92
6	5	2	NS	NS	8	NS	NS	0	NS	NS	89.2	84.30
7	4	2	-0.83	0.68	4	0.83	0.68	0	NS	NS	90.34	86.41
8	3	1	-0.83	0.69	2	0.83	0.69	0	NS	NS	93.75	91.76
9	2	1	-0.74	0.55	1	0.74	0.55	0	NS	NS	96.97	95.97

and PA difference of RF is also consistently lower than ML in all levels of classification schemes.

5.2. Relationship between class separability and overall accuracy

Both RF and ML show the same pattern of results, where there is a significant correlation between the number of class pairs with $S_{<1.0}$, $S_{1.0-1.9}$ and $S_{>1.9}$ with the resulting OA (Table 5). For Level 2 to Level 9 schemes, increasing the number of class pairs with $S_{<1.0}$ will decrease OA, while increasing the number of class pairs with $S_{>1.0-1.9}$ will increase OA. The exception is for scheme Level 1, where the OA will begin to increase if the number of class pairs with $S_{>1.9}$ increases and the increasing number of class pairs with $S_{1.0-1.9}$ actually decreases the OA. This shows that in complex classification schemes, high separability values are very important to get an increase in OA. In addition, class pairs with $S_{>1.9}$ are far more common in classes in the Level 1 scheme. This is because the description of benthic habitat classes is more detailed, so the number of classes with purer/homogeneous class statistics will be more numerous. Very few benthic habitat classes in the Level 2 to Level 9 schemes produce a value of $S_{>1.9}$ because there is already a class merging process from the Level 1 scheme. As a result, it is difficult to obtain high separability between classes because some of the classes are a combination of classes from classification schemes at the previous level, which have low separability (class statistics are mixed). The large number of benthic habitat class pairs with $S_{>1.9}$ also causes the OA results of the Level 1 classification to be comparable to the OA classification results of Levels 2–4, which has a much smaller number of classes (Zhang et al., 2013). also produced better classification accuracy with a more complex classification scheme due to the same issue.

Based on Table 5, in several classification schemes, some of the relationships between inter-class separability and OA are not significant, which is due to the limited number of samples (n for correlation analysis). However, the trends generated in the insignificant relationship are the same, i.e., negative correlations for increasing the number of $S_{<1.0}$ and a positive correlation for an increase in the number of $S_{>1.0-1.9}$ in the Level 2 - Level 9 scheme. For a Level 1 scheme, a negative correlation is also obtained for an increase in the number of $S_{<1.0}$.

5.3. Benthic habitat spatial distribution

We try to compare the spatial distribution of benthic habitat from each classification algorithm. As a sample, we take the classification result with the highest OA of Level 1 scheme (26 classes) as the most complex schemes and Level 7 (4 classes) as the most used schemes (Fig. 5). In the Level 1 classification result, it appears that the ML classification result produces very diverse class variations while RF has less variations. Briefly, it appears that ML is able to present benthic habitat variation better than RF even though the OA is far below RF. This is because ML tends to overestimate in classifying mixed benthic habitat classes, which is indicated by PA values higher than UA in 76% of total mixed benthic habitat classes, while for non-mixed classes, such as coral reef, seagrass, macroalgae, and sand, the UA value is higher than PA. Meanwhile, the UA and PA values from the RF classification results are very balanced so that there is not much overestimation or underestimation in each benthic habitat class. However, the results of the RF also tend to classify the pixels to the class with a greater number of training areas, so the area that appears dominant are those classes, e.g., macroalgae, sand, and coral reef. In the Level 7 classification result, the main difference is in the area and spatial distribution of sand and coral reef in the lagoon and back reef area of the west side of the island. The sand class on the ML result overestimated in the back reef area while the RF result overestimated the area and the spatial distribution of coral reef in the lagoon area, where the sand, which is located in between the coral reef, is generalized entirely to the coral reef class. The spatial distribution of macroalgae and seagrass in ML and RF is not much different, except in the south east side of the island, where the spatial distribution of macroalgae is in reef flat and reef cut is overestimated. These patterns are important notes in utilizing the results of classification, both from ML and RF, for subsequent uses such as in support of coastal and small island management.

6. Discussions

Many other studies have employed quite complex classification schemes and resulted in varying degrees of accuracy (Phinn et al., 2012)

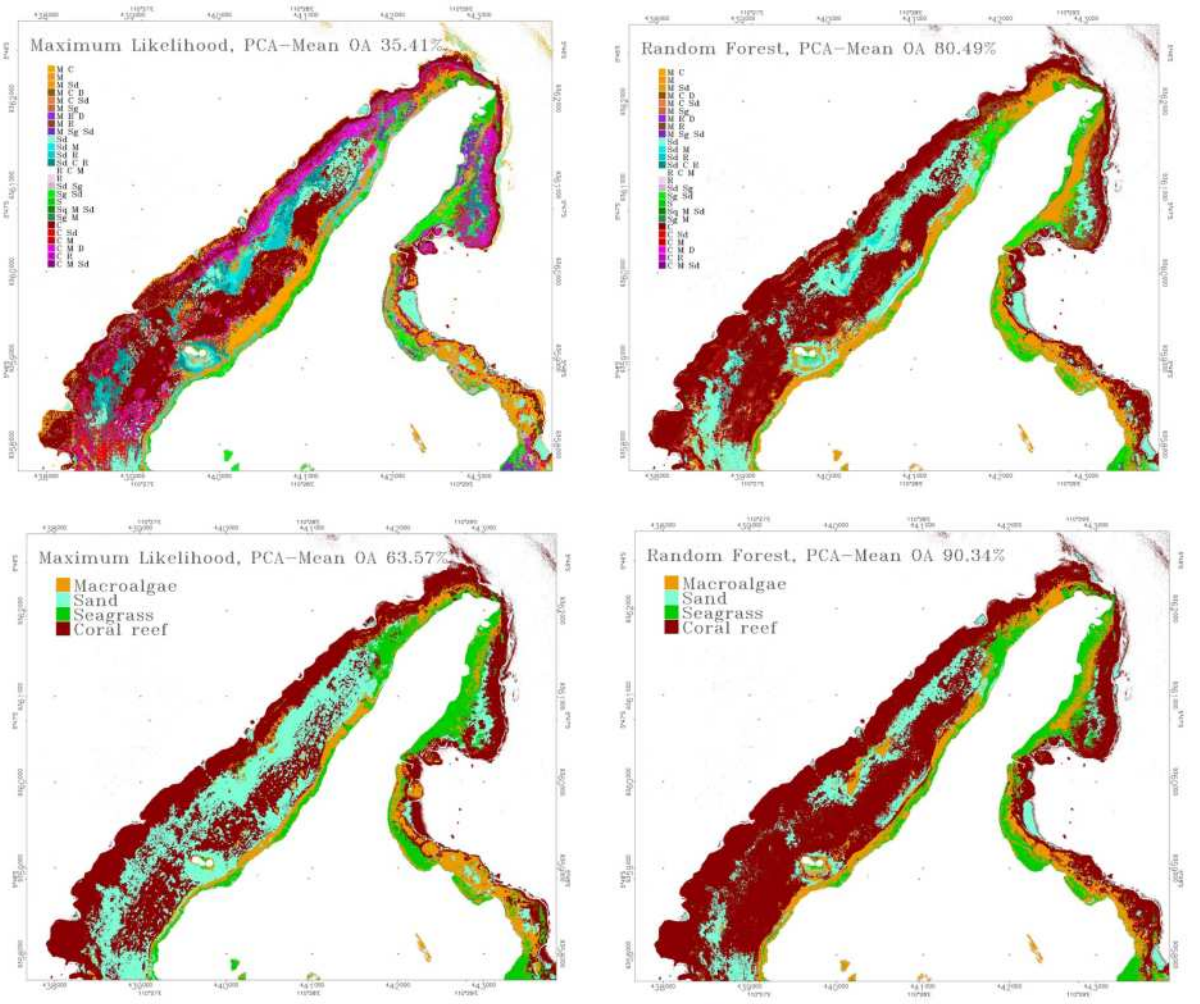

Fig. 5. Classification of benthic habitats using ML and RF at Level 1 and Level 7. Please refer to Table 4 for a description of benthic habitat classes in the legend of Level 1 schemes.

(Zhang et al., 2013) (Wicaksono et al., 2019) (Kutser et al., 2020). The variations of the classification scheme are generally caused by the demands of the purpose of the mapping application, image and methodology testing, or to represent the variation of the habitat *in-situ*. To accommodate the complexity of benthic habitat classes, previous researchers applied advanced image corrections and classifications, such as using hierarchical mapping using OBIA, from coral reefs types, reef morphology, to major and detailed ecological class (Phinn et al., 2012). The resulting OA reached more than 70% for the detailed classes. Meanwhile (Wicaksono, 2016), obtained lower accuracy for detailed mapping of benthic habitat using parametric per-pixel classification but obtained higher accuracy when using machine learning algorithms (Wicaksono et al., 2019). Nevertheless, quite a few researchers are still using the conservative benthic habitat class (e.g., four class) in their mapping activities, generally due to the mapping requirement and limited resolutions of remote sensing data used, especially multispectral images (Green et al., 2000) (Mohamed et al., 2018). However, research that discusses the extent to which the ability of the spectral resolution of remote sensing images can be used to distinguish the complexity of benthic habitat cover and how the spectral similarities between benthic habitat classes will affect the classification accuracy is still limited. This is especially true regarding benthic habitat mapping, where obtaining optimal and evenly distributed field data for many benthic habitat classes is very challenging. In this study, we assessed the relationship of inter-class spectral separability in different benthic habitat classification schemes and the resulting OA in a 2 m spatial resolution W2 image.

Our results show that inter-class separability and the number of classes affected the OA of classification results, in our case from both the RF and ML algorithm. However, RF was able to produce more consistent OA on different input types compared to ML. Nevertheless, the pattern of relationship between spectral separability and OA in RF and ML is similar. Generally, more inter-class spectral separability with $S_{<1.0}$ reduced the OA and more with $S_{1.0\text{-}1.9}$ increased the OA. This pattern, however, did not apply for the Level 1 scheme as the most complex classification scheme. An improvement in the OA of Level 1 scheme requires an increased amount of inter-class spectral separability with $S_{>1.9}$. In this scheme, the possibility of obtaining class pairs with $S_{>1.9}$ is higher since the training area statistics of the classes consist of very specific benthic composition and it is required to improve the OA. This can be a good justification for the requirement to obtain good sample distribution between classes when intending to map complex benthic habitat classes.

The issue we faced in this research is the uneven and unbalanced distribution of training areas for each benthic habitat class (Table 4). In Level 1 to Level 3 schemes, the difference in the number of training areas for each benthic habitat class is quite high. This difference directly affects the UA, PA, and spatial distribution of the resulting benthic habitat class. Here, machine learning RF is far better than the types of parametric classification, such as ML, in terms of the capability to handle classification with high number of classes, uneven training area between classes and low inter-class separability, consistency of OA on various input types, changes in the OA with increasing complexity of the classification scheme, and the consistency of UA and PA values in each classification scheme. Our work also implicitly shows the inferiority of parametric classification to a non-parametric classification algorithm to map benthic habitat, which is also in line with previous works (Zhang et al., 2013) (Wicaksono et al., 2019).

An additional finding from the results revealed that the more complex the classification scheme, the less accurate the classification gets, which was also encountered by (Andréfouët et al., 2003) and (Pu et al., 2012). One of the main factors affecting the OA is the classification schemes used, which are constructed based on the ecological variation of benthic habitats. Furthermore, there is a gap between the ecological information of benthic habitat in the field with the spectral response recorded by the sensor. We suggested that this gap is caused by the resolutions of remote sensing data used, (1) the spatial resolution — generalizing the spectral response of benthic habitat to a certain extent by pixel size, (2) the spectral resolution — capable of only recording the spectral response of benthic habitat at certain wavelengths, (3) the radiometric resolution — affects the precision of recorded spectral response, and (4) the temporal resolution — allows for differences between the information obtained during field surveys and image acquisition date. In addition, the accuracy of a particular class may significantly change when classified at different level of scheme. This is because, despite the same label, the statistics for the training area of the class changed due to the class merging. These gaps were added with several technical issues, such as the differences between image geometric accuracy and GPS accuracy, and changes of image radiometric quality during processing (Joyce et al., 2013).

Therefore, to map benthic habitats, it is necessary to check in advance whether the purpose of the mapping can be handled by the available remote sensing data and the classification methods to be used. In this context, if we want to map benthic habitat in detail and with many classes, it is recommended to use a machine-learning algorithm, especially if the amount of training area in each benthic habitat class is not balanced. It is also recommended to remain as optimal as possible in obtaining an even distribution of training areas for each class. This can be prepared from the beginning before the field survey through the selection of transect locations by considering the factors that really affect the variation of benthic habitat in the field.

7. Conclusions

This study has demonstrated that inter-class separability of benthic habitat classes in a classification scheme has an influence on the OA of the classification results and the impact is stronger on parametric classification, such as ML, than on non-parametric machine-learning classification such as RF. RF is able to handle classification with high number of classes, uneven training area distribution between classes and low separability using any input bands. This has been proven in many details of benthic habitat classification schemes. In general, an increase in the number of class pairs with $S_{<1.0}$ will decrease the OA and an increase in the number of class pairs with $S_{>1.0\text{-}1.9}$ will increase the OA. Especially for scheme Level 1, with the greatest number of classes, to increase the OA, it is necessary to increase the number of class pairs with $S_{>1.9}$. This implies that the use of detailed classification schemes requires a high degree of inter-class spectral separability to get increased OA. Therefore, while obtaining high OA is still possible with low spectral-separability class pairs, it is still necessary to ensure that the training area for each class should be able to produce high spectral separability as it indeed improved the OA, UA, and PA of the classification result, especially with a complex classification scheme.

CRediT authorship contribution statement

Pramaditya Wicaksono: Conceptualization, Methodology, Software, Validation, Formal analysis, Investigation, Resources, Data curation, Writing - original draft, Writing - review & editing, Visualization, Supervision, Funding acquisition. **Prama Ardha Aryaguna:** Methodology, Software, Validation, Writing - review & editing.

Declaration of competing interest

The authors declare that they have no known competing financial interests or personal relationships that could have appeared to influence the work reported in this paper.

Acknowledgments

We would like to thank DigitalGlobe, Inc. and Prof. Stuart Phinn from The University of Queensland for providing us the WorldView-2 image of Kemujan Island. We also thank Muhammad Hafizt from Research Center for Oceanography (P2O), Indonesian Institute for Sciences (LIPI) for assisting us during field survey.

References

Andréfouët, S., Kramer, P., Torres-Pulliza, D., Joyce, K.E., Hochberg, E.J., Garza-Perez, R., Muller-Karger, F.E., 2003. Multi-site evaluation of IKONOS data for classification of tropical coral reef environments. Rem. Sens. Environ. 88 (1–2), 128–143.

Anys, H., Bannari, A., He, D.C., Morin, D., 1994. Texture analysis for the mapping of urban areas using airborne MEIS-II images. In: Proceedings of the First International Airborne Remote Sensing Conference and Exhibition, pp. 231–245 (Strasbourg, France).

Birth, G.S., McVey, G., 1968. Measuring the color of growing turf with a reflectance spectrophotometer. Agron. J. 66, 640–643.

Breiman, L., Cutler, A., 2011. Random forests – Leo Breiman and Adele Cutler. Retrieved from. www.stat-www.berkeley.edu/users/bteiman/RandomForests/.

Congalton, R.G., Green, K., 2008. Assessing the Accuracy of Remotely Sensed Data: Principles and Practices. Mapping Science. CRC Press, Boca Rotan FL.

Eugenio, F., Marcello, J., Martin, J., 2015. High-resolution maps of Bathymetry and benthic habitats in shallow-water environments using multispectral remote sensing imagery. IEEE Trans. Geosci. Rem. Sens. 53 (7), 3539–3549.

Eugenio, F., Marcello, J., Martin, J., Rodríguez-Esparragón, D., 2017. Benthic habitat mapping using multispectral high-resolution imagery: evaluation of shallow water atmospheric correction techniques. Sensors 17 (11), 2639. https://doi.org/10.3390/s17112639.

Gitelson, A.A., Kaufman, Y.J., Stark, R., Rundquist, D., 2002. Novel algorithms for remote estimation of vegetation fraction. Rem. Sens. Environ. 80, 76–87.

Goodman, J.A., Purkis, S.J., Phinn, S.R., 2013. In: Phinn, S.R. (Ed.), Coral Reef Remote Sensing A Guide for Mapping, Monitoring and Management. Springer.

Green, E.P., Mumby, P.J., Edwards, A.J., Clark, C.D., 2000. In: Edwards, A.J. (Ed.), Remote Sensing Handbook for Tropical Coastal Management. Coastal Management Sourcebooks 3. UNESCO, Paris.

Hedley, J.D., Harborne, A.R., Mumby, P.J., 2005. Simple and robust removal of sunglint for mapping shallow-water Benthos. Int. J. Rem. Sens. 26 (10), 2107–2112.

Hedley, J.D., Roelfsema, C.M., Phinn, S.R., Mumby, P.J., 2012. Environmental and sensor limitations in optical remote sensing of coral reefs: implications for monitoring and sensor design. Rem. Sens. 4, 271–302.

Hochberg, E.J., Atkinson, M.J., 2000. Spectral discrimination of coral reef benthic communities. Coral Reefs 19, 164–171.

Huete, A., Didan, K., Miura, T., Rodriguez, E.P., Gao, X., Ferreira, L.G., 2002. Overview of the radiometric and biophysical performance of the MODIS vegetation indices. Rem. Sens. Environ. 83, 195–213.

Joyce, K.E., Phinn, S.R., Roelfsema, C.M., 2013. Live coral cover index testing and application with hyperspectral airborne image data. Rem. Sens. 5, 6116–6137.

Kakuta, S., Takeuchi, W., Prathep, A., 2016. Seaweed and seagrass mapping in Thailand measured using landsat 8 optical and textural image properties. J. Mar. Sci. Technol. 24 (6), 1155–1160. https://doi.org/10.6119/JMST-016-1026-4.

Kattenborn, T., Maack, J., Faßnacht, F., Enßle, F., Ermert, J., Koch, B., 2015. Mapping forest biomass from space – fusion of hyperspectral EO1-hyperion models. Int. J. Appl. Earth Obs. Geoinf. 35, 359–367.

Kay, S., Hedley, J.D., Lavender, S., 2009. Sun glint correction of high and low spatial resolution images of aquatic scenes: a review of methods for visible and near-infrared wavelengths. Rem. Sens. 1, 697–730.

Kutser, T., Hedley, J., Giardino, C., Roelfsema, C., Brando, V.E., 2020. Remote sensing of shallow waters – a 50 year retrospective and future directions. Rem. Sens. Environ. 240, 111619. https://doi.org/10.1016/j.rse.2019.111619.

Kutser, T., Vahtmae, E., Mersamaa, L., 2006. Spectral library of macroalgae and benthic substrates in Estonian coastal waters. Proc. Est. Acad. Sci. Biol. Ecol. 55 (4), 329–340.

Lantzanakis, G., Mitraka, Z., Chrysoulakis, N., 2016. Comparison of physically and image based atmospheric correction methods for sentinel-2 satellite imagery. In: Karacostas, T., Bais, A., Nastos, P. (Eds.), Perspectives on Atmospheric Sciences. Springer Atmospheric Sciences. Springer, Cham (ZG) Switzerland, pp. 255–261. https://doi.org/10.1007/978-3-319-35095-0_36.

Lyzenga, D.R., 1978. Passive remote-sensing techniques for mapping water depth and bottom features. Appl. Optic. 17, 379–383.

Manuputty, A., Gaol, J.L., Agus, S.B., Nurjaya, I.W., 2017. The utilization of depth invariant index and Principle component analysis for mapping seagrass ecosystem of Kotok island and Karang Bongkok, Indonesia. In: IOP Conf. Series: Earth and Environmental Science, vol. 54. IOP Publishing, Bogor.

Massot-Campos, L., Oliver-Codina, G., Ruano-Amengual, L., Miró-Juliá, M., 2013. Texture analysis of seabed images: quantifying the presence of posidonia Oceanica at palma Bay. *2013 MTS/IEEE OCEANS - Bergen*. Berg: IEEE 1–6. https://doi.org/10.1109/OCEANS-Bergen.2013.6607991.

Mather, P.M., Koch, M., 2011. Computer Processing of Remotely-Sensed Images: an Introduction, fourth ed. Wiley. fourth ed.

Mohamed, H., Nadaoka, K., Nakamura, T., 2018, May 17. Assessment of machine learning algorithms forAutomatic benthic cover monitoring and Mapping Using towed underwater video camera and high-resolution satellite images. Rem. Sens. 10 (5), 773. https://doi.org/10.3390/rs10050773.

Mumby, P.J., Edwards, A.J., 2002. Mapping marine environments with IKONOS imagery: enhanced spatial resolution does deliver greater thematic accuracy. Rem. Sens. Environ. 82, 248–257.

Oppelt, N., Schulze, F., Bartsch, I., Doernhoefer, K., Eisenhardt, I., 2012. Hyperspectral classification approaches for intertidal macroalgae habitat mapping: a case study in Heligoland. Opt. Eng. 51 (2).

Penuelas, J., Gamon, J.A., Griffin, K.L., Field, C.B., 1993. Assessing community type, plant biomass, pigment composition, and photosynthetic efficiency of aquatic vegetation from spectral reflectance. Rem. Sens. Environ. 46 (2), 110–118.

Phinn, S.R., Roelfsema, C.M., Mumby, P.J., 2012. Multi-scale, object-based image analysis for mapping geomorphic and ecological zones on coral reefs. Int. J. Rem. Sens. 33 (12), 3768–3797.

Pu, R., Bell, S., Meyer, C., Baggett, L., Zhao, Y., 2012. Mapping and assessing seagrass along the western coast of Florida using Landsat TM and EO-1 ALI/Hyperion imagery. Estuar. Coast Shelf Sci. 115, 234–245.

Richards, J.A., 2013. Remote Sensing Digital Image Analysis. Springer-Verlag, Berlin, Germany.

Roelfsema, C.M., Phinn, S.R., 2009. A Manual for Conducting Georeferenced Photo Transects Surveys to Assess the Benthos of Coral Reef and Seagrass Habitats. Centre for Remote Sensing & Spatial Information Science, School of Geography, Planning & Environmental Management, University of Queensland, Queensland.

Roelfsema, C., Phinn, S., Jupiter, S., Comley, J., Albert, S., 2013. Mapping coral reefs at reef to reef-system scales, 10s–1000s km2, using object-based image analysis. Int. J. Rem. Sens. 34 (18), 6367–6388.

Rouse, J.W., Haas, R.H., Schell, J.A., Deering, D.W., 1973. Monitoring vegetation systems in the great plains with ERTS. In: Third ERTS Symposium. SP-351 I. NASA, pp. 309–317.

Su, L., Huang, Y., 2009. Support vector machine classification: comparison of linkage techniques using a clustering-based method for training data selection. GIScience Remote Sens. 46 (4), 411–423.

Updike, T., Comp, C., 2010. Radiometric Use of WorldView-2 Imagery. DigitalGlobe®, Longmont, Colorado.

Wicaksono, P., 2010. Integrated Model of Water Column Correction Technique for Improving Satellite-Based Benthic Habitat Mapping, A Case Study on Part of Karimunjawa Islands, Indonesia. Universitas Gadjah Mada. Faculty of Geography, Universitas Gadjah Mada, Yogyakarta.

Wicaksono, P., 2016. Improving the accuracy of Multispectral-based benthic habitats mapping using image rotations: the application of Principle Component Analysis and Independent Component Analysis. Eur. J. Rem. Sens. 49, 433–463.

Wicaksono, P., Hafizt, M., 2013. Mapping seagrass from space: addressing the complexity of seagrass LAI mapping. Eur. J. Rem. Sens. 46, 18–39.

Wicaksono, P., Aryaguna, P.A., Lazuardi, W., 2019a. Benthic habitat mapping model and cross validation using machine-learning classification algorithms. Rem. Sens. 11 (11), 1279. https://doi.org/10.3390/rs11111279.

Wicaksono, P., Fauzan, M.A., Kumara, I.S., Yogyantoro, R.N., Lazuardi, W., Zhafarina, Z., 2019b. Analysis of reflectance spectra of tropical seagrass species and their value for mapping using multispectral satellite images. Int. J. Rem. Sens. 40 (23), 8955–8978. Retrieved from. https://www.tandfonline.com/doi/full/10.1080/01431161.2019.1624866.

Wicaksono, P., Hafizt, M., Ardiyanto, R., 2013. Initial results of remote sensing-based benthic habitat classification scheme development of Karimunjawa islands. In: Prosiding Simposium Nasional Sains Geoinformasi — III 2013. PUSPICS Fakultas Geografi UGM, Yogyakarta, pp. 233–239.

Yang, D., Yang, Y., Yang, C., Zhao, J., Sun, Z., 2011. Detection of seagrass in optical shallow water with Quickbird in the Xincun Bay, Hainan province, China. IET Image Process. 5 (5), 363–368.

Zapata-Ramirez, P.A., Blanchon, P., Olioso, A., Hernandez-Nunez, H., Sobrino, J.A., 2013. Accuracy of IKONOS for mapping benthic coral-reef habitats: a case study from the Puerto Morelos Reef National Park, Mexico. Int. J. Rem. Sens. 34 (9–10), 3671–3687.

Zhang, C., 2015. Applying data fusion techniques for benthic habitat mapping and monitoring in a coral reef ecosystem. ISPRS J. Photogrammetry Remote Sens. 104, 213–223.

Zhang, C., Selch, D., Xie, Z., Roberts, C., Cooper, H., Chen, G., 2013. Object-based benthic habitat mapping in the Florida Keys from hyperspectral imagery. Estuar. Coast Shelf Sci. 134, 88–97.

Zoffoli, M.L., Frouin, R., Kampel, M., 2014. Water column correction for coral reef studies by remote sensing. Sensors 14 (9), 16881–16931. https://doi.org/10.3390/s140916881.

1-s2.0-S2352938520300690-main_1.pdf

ORIGINALITY REPORT

15%	12%	12%	4%
SIMILARITY INDEX	INTERNET SOURCES	PUBLICATIONS	STUDENT PAPERS

MATCH ALL SOURCES (ONLY SELECTED SOURCE PRINTED)

5%

★ www.tandfonline.com

Internet Source

Exclude quotes	On	Exclude matches	Off
Exclude bibliography	On		